Chemical Physics 349 (2008) 98–108

Contents lists available at ScienceDirect

Chemical Physics

journal homepage: www.elsevier.com/locate/chemphys

Structure and energetics of InN and GaN dimers

Lucia Šimová [a], Demeter Tzeli [b], Miroslav Urban [a], Ivan Černušák [a,*], Giannoula Theodorakopoulos [b], Ioannis D. Petsalakis [b]

[a] Department of Physical and Theoretical Chemistry, Faculty of Natural Sciences, Comenius University, Mlynská dolina, SK-842 15 Bratislava, Slovakia
[b] Theoretical and Physical Chemistry Institute, The National Hellenic Research Foundation, 48 Vassileos Constantinou Avenue, Athens 116 35, Greece

ARTICLE INFO

Article history:
Received 25 January 2008
Accepted 26 February 2008
Available online 4 March 2008

This paper is dedicated to professor Hans Lischka on the occasion of his 65th birthday as the appreciation of his outstanding contribution to the developments in the field of quantum chemistry.

Keywords:
Group-III nitrides
Molecular clusters
CCSD(T) calculations
Excited states
Dissociation energies

ABSTRACT

Large-scale mapping of various dimers of indium nitride and gallium nitride in singlet and triplet electronic states is reported. Second-order perturbation theory with Møller–Plesset partitioning of the Hamiltonian (MP2) and coupled-cluster with single and double excitations corrected for the triple excitations (CCSD(T)) are used for the geometry determinations and evaluation of excitation and dissociation energies. For gallium and nitrogen we have used the singly augmented correlation-consistent triple-zeta basis set (aug-cc-pVTZ), for indium we have used the aug-cc-pVTZ-pseudopotential basis set. The dissociation energies are corrected for basis set superposition error (BBSE) including geometrical relaxation of the monomers. We compare and discuss the similarities and dissimilarities in the structural patterns and energetics of both groups of isomers, including the effect of the BSSE. Our computations show that there are not only different ground states for In_2N_2 and Ga_2N_2 but also different numbers of stable stationary points on their potential energy surface. We compare our results with the molecular data published so far for these systems.

1. Introduction

During the past decades the group-III nitrides (MeN) have been in the focus of interest in both material science [1–4] and molecular studies [5–12]. The materials based on AlN are supposed to replace silicon- or gallium–arsenide-based materials in the near future. The use of GaN and InGaN in the active layer of high-efficiency light-emitting diodes enables the emission of amber, green, blue and ultraviolet light which makes them ideal for displays and numerous other hi-tech applications [13]. With the use of gallium nitride structures white light-emitting diodes can be obtained free of electrostatic fields, resulting in dramatic reduction of power consumption with beneficial economic and ecological consequences [14]. Besides light-emitting diodes, the range of their applications is wide (short-wavelength lasers, solar cells, high-temperature/high-power electronic devices) and has made them good candidates for new-generation of opto- and microelectronic elements.

Recently, Vaddiraju and co-workers studied the formation of one-dimensional (1D) indium nitride structures using chemical vapour deposition [15]. They utilized the "reactive vapour transport" technique to synthesise InN nanowires. To explain the 1D growth of InN on a suitable substrate they proposed the mechanism which includes preferential wetting of the existing InN layer (rather than the substrate) with In atoms coming from the vapour followed by the dissolution of nitrogen into the indium droplets. This is an interesting idea since it implicitly presumes the existence of a mixture of indium–nitrogen clusters of various size and composition.

To understand the properties of the electronic devices based on group-III nitrides at microscopic level and utilize their full potential in material applications, it is necessary to investigate the link between the molecular world (represented by isolated species) and the solid state (typically represented by one-dimensional nanowires or thin films). The importance of nano-clusters is closely related to the degree of minimization of the building blocks of integrated circuits. Various modifications of electron microscopy technique allow one to manipulate the materials and surfaces at molecular or even atomic level. Thus, the physical and chemical properties of the clusters based on diatomic dimers, trimers, etc., are of interest. For example, a preparation of the material for electronic devices generally involves either chemical vapour deposition [16] or the sputtering of the metal atom in the presence of nitrogen to make thin layers of MeN [17]. In both cases one can not avoid the existence of surface defects. The microstructures representing these defects can be viewed as the clusters of MeN adsorbed on a thin film [18,19].

* Corresponding author. Tel.: +42 1260296429; fax: +42 1265429064.
E-mail addresses: cernusak@fns.uniba.sk (I. Černušák), ithe@eie.gr (G. Theodorakopoulos).

0301-0104/$ - see front matter © 2008 Elsevier B.V. All rights reserved.
doi:10.1016/j.chemphys.2008.02.051

There are only three studies on structures and relative energies of In_2N_2. Cardelino et al. calculated a series of compounds containing In atoms using the DFT method [7]. Only two structures of the In_2N_2 molecule, a linear $^3\Sigma_g$ ($D_{\infty h}$), which was their most stable and a rhombic (D_{2h}) were examined in their work utilizing the B3LYP functional. Costales et al. have performed a DFT study of the structure, stability, vibrational frequencies and ionization energies of five singlet and triplet structures of In_2N_2 [5] and analyzed the character of their chemical bonding [6]. Their lowest energy was calculated for the $^3\Sigma$ linear InInNN structure ($C_{\infty v}$) which shows one imaginary frequency. The rhombic D_{2h} singlet structure was more stable than the linear InNNIn $D_{\infty h}$ structure, in contrast to Ref. [7]. Finally, a recent paper by Cao and Balasubramanian [8] comprises 20 In_2N_2 species having different geometries and multiplicities. This time, the most stable structures were T-shaped. All structures and energies have been computed by the MRCI method combined with the relativistic effective core potentials for the core electrons of In and N atoms with (4s4p1d) basis set for the outer $5s^25p^1$ shells for the In atom and the outer $2s^22p^3$ for the N atom [8].

Very little is known about dimers of Ga_2N_2. Since both GaN and InN molecules and their clusters can be considered as species important in opto-electronics and other applications, it is interesting to compare properties of these molecules by using analogous methods. To our knowledge the only work which allows comparisons of the relative stability of In_2N_2 and Ga_2N_2 molecules (and, in addition, Al_2N_2 clusters) was published by Kandalam et al. [5,6]. Only two structures of Ga_2N_2 in their study are true minima, namely a rhombic, (^1A_g, D_{2h}), their global minimum, and a linear triplet state of the GaNGaN structure, $D_{\infty h}$. The remaining three linear triplet state structures have an imaginary frequency. This should be compared with their In_2N_2 complexes which have three minima (a rhombic and two linear, InNInN and the InNNIn structures). T-shaped structure of In_2N_2 and Ga_2N_2 were not considered in the work of Kandalam et al. [5,6]. As it is shown in Ref. [8] such structures are the most stable structures of In_2N_2. Limited number of structures optimized at B3LYP/6-311+G* level was mentioned by Zhou and Andrews in their laser-ablation study [20]. They reported only three structures – rhombic singlet (^1A_g) and triplet (^3A_u) and linear $^3\Sigma_u^-$ GaNNGa triplet.

We have decided to extend previous studies of both In_2N_2 and Ga_2N_2 molecules by using high-level CCSD(T) calculations which allow comparison of both molecules. Previously, we have studied relative stabilities of Ga_2N and GaN_2 clusters as well as the adsorption of Ga, GaN, GaN_2 and their cations at a silicon surface [21]. In this respect the present calculations are complementary to our previous work. One of the reasons for using CCSD(T) methods is accuracy. Bonding in GaN and InN complexes extends from weak Van der Waals (VdW) interactions up to relatively strong chemical bonding. DFT methods which are unavoidable when larger complexes and surface bonding are considered have difficulties in describing particularly the VdW interactions and so the comparison of different structures may be not accurate enough. Finally, even if the sequence of stabilities of In_2N_2 complexes calculated by DFT and wave function methods [5,8] is similar in a few complexes for which comparison is possible, excitation energies differ by as much as by 0.5 eV. We believe that more accurate analysis of these and similar clusters in terms of geometries, electronic structure, energetics and vibrational frequencies can assist in the interpretation of experimental data and future design of the materials. The aim of present work is, therefore, more accurate investigation of above mentioned molecular properties of the different Me_2N_2 isomers in their ground and selected low-lying excited states. Using these data we want to (1) indicate the weakest bonds in the clusters, (2) analyze the potential fragments originating from Me_2N_2 once these clusters are physi- or chemisorbed on the solid state surface (e.g. silicon), in future work. In this paper we consider the following potential fragments: MeN, Me_2, N_2 and/or atoms Me, N.

As indicated by several theoretical studies, numerous possible structures and/or electronic states may be considered both for monomers [22,23] and for higher clusters [5,6,8,9]. In this study we have restricted ourselves to the lowest singlet and triplet states. Section 2 gives the details of the basis sets and computational approaches employed. The results for both In_2N_2 and Ga_2N_2 are presented and discussed in Section 3. In Section 4 we compare with previous work on the two systems and summarize our results.

2. Calculations

We have performed geometry optimizations for the In_2N_2 and Ga_2N_2 isomers for various electronic states displayed in Fig. 1. Some of the structures from Fig. 1 were also considered by Costales et al. in their DFT study of Ga_2N_2 dimers [5] and by Cao and Balasubramanian in the MRCI study of In_2N_2 [8].

The optimizations were carried out using the Gaussian03 [24] package and the reference wave function was RHF (for singlets) and UHF (for triplets). Optimal geometries were obtained at the second-order Møller–Plesset perturbation theory (MP2) [25]. For gallium we have used the singly augmented correlation-consistent basis set of triple-zeta quality (MP2/aug-cc-pVTZ level), for indium we have used aug-cc-pVTZ-PP basis [26–29]. The latter employ an accurate small-core ($1s^22s^22p^63s^23p^63d^{10}$, i.e. 28 electrons) relativistic pseudopotentials and a (13s12p10d2f) → [6s5p4d2f] basis set for the remaining electrons, $4s^24p^64d^{10}5s^25p^1$. Thus a total of 202 contracted Gaussian functions have been employed for In_2N_2 and 210 contracted Gaussian functions for Ga_2N_2. In the MP2 calculations the $2s^22p^3$ electrons of the N atom, the $4s^24p^64d^{10}5s^25p^1$ electrons of In and $3s^23p^63d^{10}4s^24p^1$ electrons of Ga were correlated. Thus, for both molecules 52 electrons were correlated in the MP2 step. In the RCCSD(T) calculations the $2s^22p^3$ electrons of *N*, the $4d^{10}5s^25p^1$ of In and $3s^23p^63d^{10}4s^24p^1$ electrons of Ga were correlated. Thus, in the RCCSD(T) step 36 electrons of In_2N_2 and 52 electrons of Ga_2N_2 were correlated. In total, we have determined 28 structures for In_2N_2 and 22 structures for Ga_2N_2 They include different space and/or spin symmetries involving eleven different linear, T-shaped, rhombic and planar structures corresponding to minima or transition states. All optimized species were subject to a harmonic frequency check to discriminate between minima and transition states. The resulting geometries (equilibrium distances, bond angles) and energy orderings are reported for all the structures in the next section, while the harmonic frequencies are provided separately as Supplementary material. The other details of the calculations are collected in Table 1.

Optimal geometries served as an input for single-point calculations of (restricted Hartree–Fock single-reference) RCCSD(T)/aug-cc-pVTZ energies (the acronym RCCSD(T) stands for coupled-clusters with single and double excitations corrected for the triple excitations) [30–33]. Usually, the use of MP2 geometries for the single-point RCCSD(T) energies leads to significant change in energy ordering of isomers and/or singlet/triplet separations over the MP2 ones. For some isomers, where we have found large mono- and bi-excitation amplitudes from the CCSD computational step (see next paragraphs) we have repeated the geometry optimization also at RCCSD(T)/aug-cc-pVTZ level. In the case of the In_2N_2 all the reported RCCSD(T) results have been obtained after a geometry optimization.

We note that both approaches, MP2 and RCCSD(T) use as a reference wave function the Hartree–Fock solution of SCF equations of molecular problem. We have used MOLCAS 6.5 [34] package

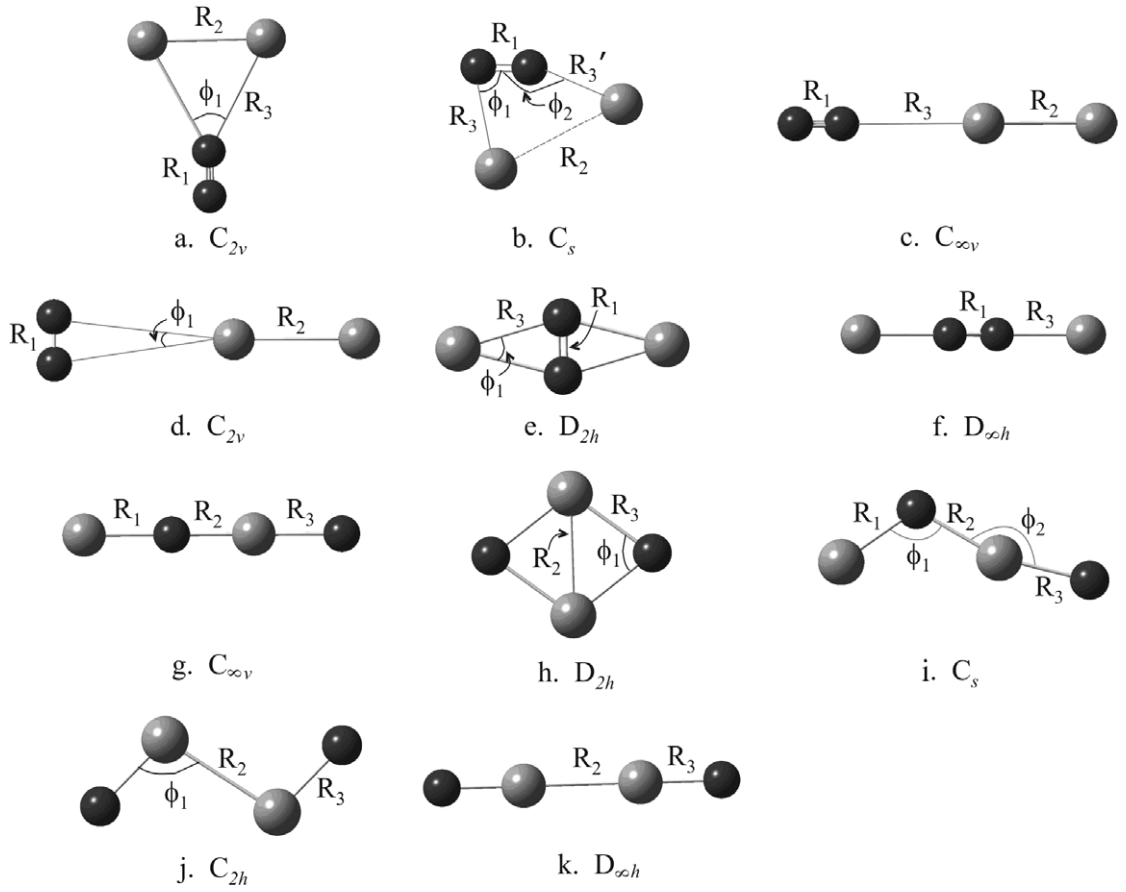

Fig. 1. Calculated structures of the Me_2N_2 molecules.

Table 1
Details of the calculations

Atom	Basis	Correlated electrons	Note
Nitrogen	aug-cc-pvtz	2s, 2p	
Gallium	aug-cc-pvtz	3s, 3p, 3d, 4s, 4p	
Indium	aug-cc-pvtz-PP	4s, 4p, 4d, 5s, 5p	MP2 step
		4d, 5s, 5p	RCCSD(T) step[a]

[a] The CC calculation with more correlated electrons (+4s4p) was unstable.

The energetics of the In_2N_2 and Ga_2N_2 isomers can be investigated from two points of view. First, we can look at the relative ordering of the isomers in both singlet and triplet states. Secondly, we can define and compute the dissociation energies D_i of the cluster related to selected products of dissociation (Me = Ga, In):

$$Me_2N_2 \rightarrow Me_2 + N_2 \qquad D_1 \tag{1}$$
$$Me_2N_2 \rightarrow 2Me + N_2 \qquad D_2 \tag{2}$$
$$Me_2N_2 \rightarrow 2MeN \qquad D_3 \tag{3}$$

for the Ga_2N_2 and MOLPRO2006 for the In_2N_2 calculations of the final energies. In this part of our work, the reference wave functions were RHF (for singlets) and ROHF (for triplets).

Since we are dealing with yet unknown species and we are using the single-reference RCCSD(T) method, it is useful to analyze carefully the Hartree–Fock stability of the SCF solution as well as the final mono- and bi-excitation amplitudes from the CCSD computational step. Large amplitudes may: (1) either signal large sensitivity of the geometry of particular dimer with respect to the method (in other words – the inadequacy of the assumption that MP2 geometry can be used in RCCSD(T) calculation); (2) or indicate the existence of a multireference problem, which is for large mono-excitation amplitudes often accompanied with Hartree–Fock instability. To alleviate the first possibility we have repeated the optimization of the geometry of some clusters also at the RCCSD(T)/aug-cc-pVTZ level. In favourable cases, the refinement at RCCSD(T) lowers the excitation-amplitudes because the system relaxes to less stretched bonds (it is known that the MP2 method tends to overestimate bond lengths [31]).

Table 2
Absolute values of the largest t_1 and t_2 amplitudes from RCCSD(T)/aug-cc-pVTZ calculations of Ga_2N_2 and In_2N_2

Species	Ga_2N_2		In_2N_2	
	$\|t_1\|$	$\|t_2\|$	$\|t_1\|$	$\|t_2\|$
^{1}**6a**	<0.05	0.090	<0.05	0.106
^{1}**9c**	<0.05	0.094	<0.05	0.108
^{1}**17h**	0.100	0.075	0.150	0.103
^{3}**19h**	0.105	0.088	0.153	0.091
^{3}**21g**[a]	0.177	0.028	0.067	0.054
^{3}**25j**[a]	0.187	0.077	–	–
^{3}**27k** ($^3\Sigma_g^+$)	0.184	0.079	–	–
^{3}**11b**	0.101	0.038	0.371	0.061
^{3}**15g**	–	–	0.329	<0.05
^{1}**22g**	0.298	0.110	–	–
^{1}**26g**	–	–	0.351	0.247
^{3}**23h**	0.124	0.240	0.138	0.149

Only structures with at least one amplitude larger than 0.1 are given.
[a] The largest t_1 amplitudes of GaN fragments needed for BSSE corrections to reaction energies of the ^{3}**21g**, and ^{3}**25j** structures are 0.23 and 0.22, respectively.

The first reaction refers to the stability of Me_2N_2 considered as a product of dimerization of the two homonuclear monomers. The second one can be described as the interaction of nitrogen molecule with two Ga or In atoms and the third is the dimerization of heteronuclear monomers. In each case one has to be careful in the evaluation of the relative energies within a supermolecule approach. Our aug-cc-pVTZ basis set is flexible enough and thus appropriate for geometry determinations, however, it is still not saturated for energy evaluations. Thus, the energy differences arising from Eqs. (1)–(3) may be affected by the basis set superposition error (BSSE). Therefore, in the evaluation of the binding energies we estimated the BSSE using the counterpoise correction [35,36] considering the geometry relaxation. This requires calculations of the supersystem and all subsystems in the supersystem geometry with the supersystem basis set, as well as calculations of the subsystems in their respective basis sets with both the geometry corresponding to the supersystem and to the geometry of the separated subsystem, respectively.

3. Results

We have considered 11 geometries for both systems (Fig. 1). Typically, the actual number of the conceivable In_2N_2 or Ga_2N_2 isomers is higher since each geometrical structure can acquire various electronic states. For convenience the isomers have been labeled by three symbols, the first indicating the spin multiplicity (superscript 1 or 3), the second the energy rank of the isomer at the MP2 level of theory, and the third is the structural type according to Fig. 1. For example, ^{3}**1a** is the triplet state for the lowest (most stable) T-shaped structure **a**. Note that not all structures listed for In_2N_2 could be also optimized for Ga_2N_2. In addition, Ga_2N_2 dimers having energies very high above the minimum energy have been omitted. In some electronic states and geometry structures, as listed in Table 2, high t_1 or t_2 CCSD excitation amplitudes of In_2N_2 or Ga_2N_2 were detected. High CCSD amplitudes indicate that a molecule under consideration is not adequately described by CCSD with a single-determinant reference. According to our expe-

Table 3
MP2 geometries and ordering of the In_2N_2 isomers

Species/sym/state/type[a]				R_1	R_2	R_3	ϕ_1	ϕ_2	T_e
^{3}**1a**	C_{2v}	$^3B_1$	m	1.112	2.918	3.124	55.7		0.0
				1.104	2.981	3.241	54.8		0.0
^{1}**2b**	C_s	$^1A'$	m	1.188	3.254	2.470, 2.332[b]	77.9	159.0	0.103
				1.11	3.26	3.46, 2.95[b]	71.0	153.0	0.294
^{3}**3c**	$C_{\infty v}$	$^3\Sigma^-$	m	1.114	2.728	3.435			0.186
				1.104	2.774	3.607			0.206
^{3}**4d**	C_{2v}	$^3B_2$	TS	1.114	2.951	4.259	15.0		0.192
				1.104	3.004	4.462	14.2		0.120
^{3}**5d**	C_{2v}	$^3A_2$	TS	1.115	2.714	3.812	16.8		0.224
				1.104	2.769	3.987	15.9		0.235
^{1}**6a**	C_{2v}	$^1A_1$	m	1.124	2.739	2.711	55.3		0.432
				1.106	2.834	3.054	60.7		0.487
^{1}**7e**	D_{2h}	^1A_g	m	1.250		2.330	31.1		0.553
				1.250		2.345	30.9		0.715
^{1}**8d**	C_{2v}	$^1A_1$	TS	1.114	3.249	4.524	14.1		0.584
				1.104	3.289	4.708	13.5		0.374
^{1}**9c**	$C_{\infty v}$	$^1\Sigma^+$	TS	1.115	2.772	3.215			0.707
				1.104	2.858	3.584			0.610
^{3}**10f**	$D_{\infty h}$	$^3\Sigma_g^-$	m	1.165		2.210			1.047
				1.191		2.170			1.183
^{3}**11b**	C_s	$^3A''$	m	1.179	3.661	2.284, 2.243[b]	83.9	169.8	1.187
				1.21	2.96	2.62, 2.37[b]	75.0	151.0	1.090
^{1}**12f**	$D_{\infty h}$	$^1\Sigma_g^+$	m	1.172		2.242			1.189
				1.176		2.233			1.412
^{3}**13a**	C_{2v}	$^3A_2$	m	1.135	2.996	2.439	75.8		1.748
^{3}**14e**	D_{2h}	$^3B_{2g}$	m	1.298		2.293	32.9		1.853
^{3}**15g**	$C_{\infty v}$	$^3\Sigma^-$	TS[c]	2.028	1.885	2.094			4.222
				2.098	1.923	1.982			5.092
^{3}**16h**	D_{2h}	$^3B_{3u}$	N/A[d]		3.170	2.070	99.9		4.893
^{1}**17h**	D_{2h}	^1A_g	m		2.622	2.170	74.3		5.145
					2.699	2.180	76.5		6.055
^{3}**18i**	C_s	$^3A''$	m	2.015	2.029	1.974	113.8	162.8	5.742
^{3}**19h**	D_{2h}	$^3B_{1g}$	TS		2.730	2.110	80.6		5.761
					2.783	2.157	80.3		5.275
^{3}**20g**	$C_{\infty v}$	$^3\Sigma^+$	N/A[d]		–	–	–		–
					2.120	2.031	1.979		5.671
^{3}**21g**	$C_{\infty v}$	$^3\Pi$	m	1.980	1.854	1.989			5.946
				1.946	1.944	1.995			5.717
^{1}**22g**	$C_{\infty v}$	$^1\Sigma^+$	m	2.060	1.878	2.027			6.223
^{3}**23h**	D_{2h}	$^3B_{1u}$	m		–	–	–		–
					3.116	2.144	93.2		6.524
^{1}**24j**	C_{2h}	^1A_g	m		2.756	1.923	101.3		6.620
^{3}**25j**	C_{2h}	^3B_g	m		2.546	2.049	158.3		8.486
^{1}**26g**	$C_{\infty v}$	$^3\Sigma^+$	m	1.932	1.965	1.917			8.528
				1.875	1.941	1.855			
^{3}**27k**	$D_{\infty h}$	$^1\Sigma_g^-$	TS[c]		2.504	2.026			8.530
^{1}**28k**	$D_{\infty h}$	$^1\Sigma_g^+$	m		2.460	1.792			10.313

For some species also the RCCSD(T) geometries and excitation energies are given as a second row for the pertinent structure. Distances in Ångstrom, angles in deg, T_e's in eV.

[a] m = minimum, TS = transition state, TS_2 = second-order transition state.

[b] Bond length R_3' (Fig. 1).

[c] Two degenerate imaginary linear bends.

[d] Frequency calculation failed.

rience (see, e.g. [37]), single-determinant CCSD(T) can be safely used when amplitudes are smaller than 0.1. Results with amplitudes not exceeding absolute value of 0.2 are still acceptable, but calculations having CCSD amplitudes higher than 0.2 should be taken with caution or, even better, should be omitted. Such amplitudes indicate quasidegeneracy problems and respective species must be calculated by much more complicated and time demanding multireference CC or CI methods. Geometries and excitation energies of some such structures of In_2N_2 are listed in Table 3. The bond lengths and the dissociation energies of the In_2, N_2 and InN are given in Table 4. We have listed all optimized In_2N_2 structures in Table 3 for the sake of completeness, but not all have been considered in fragmentation reactions, Tables 5–7. Analogously, geometry data and excitation energies of different isomers of Ga_2N_2 and the respective monomers are collected in Tables 8 and 9 and the corresponding reaction energies are summarized in Tables 10–12.

Following Eqs. (1)–(3) the calculated structures can be divided into three categories according to their possible fragments, $Me_2 + N_2$, $2Me + N_2$ or $2MeN$. In subsequent sections we present separately the results for In_2N_2 and for Ga_2N_2 (geometries and energetics). The dissociation energies in Tables 5–7, 10–12 are arranged according to the magnitude of the excitation energy of the particular isomer, as presented in the last column of Tables 3 and 8. The harmonic frequency wave numbers and IR intensities are available in Supplementary material.

To simplify the discussion, we will present the In_2N_2 first because the number of stable indium nitride isomers is larger than those for gallium nitride. This will make the comparison of the isomers ordering more transparent.

Table 4
Bond lengths R_e (Å), dissociation energies D_e (kJ/mol) with respect to the ground state products of In_2, N_2 and InN molecules, harmonic frequencies ω_e (cm^{-1}) and excitation energies T_e (eV) at MP2 and RCCSD(T)/aug-cc-pVTZ(-PP) levels of theory

Species	MP2				RCCSD(T)		
	R_e	D_e	ω_e	T_e	R_e	D_e	T_e
$In_2(X^3\Pi)$	2.953	129.0	127.6	0.0	3.005	119.4	0.000
$In_2(A^3\Sigma_g^-)$	2.709	123.8	166.9	0.050	2.770	107.3	0.125
$In_2(a_1\Sigma_g^+)_G$ [a]	3.251	91.37	101.6	0.390	3.290	94.9	0.254
$In_2(a1\Sigma_g^+)_L$ [a]	2.764	71.8	150.1	0.593	2.858	68.3	0.530
$InN(X^3\Sigma^-)$	2.191	165.1	494.7	0.0	2.222	166.4	0.000
$InN(A^3\Pi)$	2.067	136.5	600.1	0.296	2.084	145.7	0.214
$N_2(X^1\Sigma_g^+)$	1.114	964.9	2186.2	0.0	1.104	913.2	–

[a] G = Global, L = Local minimum.

Table 5
Dissociation energies D_1 (kJ/mol) with respect to $In_2(X^3\Pi) + N_2(X^1\Sigma_g^+)$ for the triplet and $In_2(a^1\Sigma_g^+) + N_2(X^1\Sigma_g^+)$ for the singlet structures of the In_2N_2 molecule, D_2 with respect to $2In(^2P) + N_2(X^1\Sigma_g^+)$

Species	D_1	$D_{1(BSSE)}$ [a]	D_2 [b]	$D_{2\ (BSSE)}$ [a]
	$\rightarrow In_2 + N_2$		$\rightarrow 2In + N_2$	
	22.0	8.7	151.0	118.9
	13.7	6.3	133.2	115.6
	4.1	−2.0	133.1	102.6
	−6.1	−9.4	113.3	98.1
	3.5	0.7	132.5	111.1
	2.1	0.7	121.6	110.2
	0.4	−11.6	129.4	100.9
	−9.0	−11.5	110.4	95.0
	17.9	−6.3	109.3	76.6
	−8.8	−18.8	86.2	64.6
	3.4	1.3	94.7	78.7
	2.2	0.7	97.1	85.8
	−46.2	−52.3	82.8	52.2
	−20.7	−24.1	74.3	60.4
	[c]		[c]	

For each isomer the first row refers to MP2/aug-cc-pVTZ, the second row refers to RCCSD(T)/aug-cc-pVTZ level of theory.
[a] BSSE-corrected value.
[b] The $^2P_{1/2} \rightarrow {}^2P_{3/2}$ excitation energy for indium is 0.274 eV (experiment [41]), or 0.261 eV (CASPT2/SOC calculation [42]).
[c] Unbound.

Table 6
Dissociation energies D_2 (kJ/mol) with respect to $2In(^2P) + N_2(X^1\Sigma_g^+)$ of different species of the In_2N_2 molecule

Species		D_2	$D_{2\ (BSSE)}$ [a]
		$2In + N_2$	
	^{1}**2b**	141.1	85.7
		104.8	89.8
	^{1}**7e**	97.6	35.9
		64.2	28.3
	^{3}**10f**	50.0	−9.9
		9.1	−24.8
	^{1}**12f**	36.3	−20.9
		−3.1	−34.3
	^{3}**14e**	[b]	[b]

For each isomer the first row refers to MP2/aug-cc-pVTZ, the second row refers to RCCSD(T)/aug-cc-pVTZ level of theory.
[a] BSSE-corrected value.
[b] Unbound.

Table 7
Dissociation energies D_3 (kJ/mol) with respect to $2InN(X^3\Sigma^-)$ of the In_2N_2 molecules

Species		D_3	$D_{3\ (BSSE)}$ [a]
		2InN	
	^{3}**16h**	313.6	254.4
	^{1}**17h**	289.3	227.8
		129.4	101.3
	^{3}**18i**	231.7	190.8
	^{3}**19h**	229.8	168.4
		204.6	171.3
	^{3}**21g**	212.0	157.7
		162.0	143.6
	^{1}**22g**	185.3	134.7
	^{1}**24j**	147.0	119.4
	^{3}**25j**	[b]	[b]
	^{3}**27k**	[b]	[b]
	^{1}**28k**	d	[b]
	^{3}**20g**[c]	184.5	170.5
	^{3}**23h**[c]	102.2	71.0

The first row refers to MP2/aug-cc-pVTZ, the second (optional) row refers to RCCSD(T)/aug-cc-pVTZ level of theory.
[a] BSSE-corrected value.
[b] Unbound.
[c] Minimum found only at the CCSD(T) level.

Table 8
Geometries of the Ga_2N_2 isomers and RCCSD(T) excitation energies T_e

Species/sym/state/type[a]				R_1	R_2	R_3	ϕ_1	ϕ_2	T_e
^{1}7e	D_{2h}	^1A_g	m	1.284	2.077	36.0			
				2.084	35.8		0.000		
^{3}1a	C_{2v}	$^3B_1$	TS	1.104	2.511	2.630	57.0	0.174	
^{1}2b	C_s	$^1A'$	m	1.198	2.755	2.300, 2.166[b]	77.4	145.9	0.214
^{3}3c	$C_{\infty v}$	$^3\Sigma^-$	TS[c]	1.114	2.443	3.613			0.355
^{3}5d	C_{2v}	$^3A_2$	TS_2	1.114	2.436	3.973	16.1		0.384
^{3}4d	C_{2v}	$^3B_2$	TS	1.114	2.577	4.119	15.6		0.396
^{3}10f	$D_{\infty h}$	$^3\Sigma_g^-$	m	1.189		1.933			
				1.200		1.930			0.502
^{1}6a	C_{2v}	$^1A_1$	m	1.145	2.345	2.235	63.3		0.533
				1.220	3.265	2.065, 1.955[b]	80.1	147.9	0.790
^{1}8d	C_{2v}	$^1A_1$	TS	1.115	2.404	3.662	17.5		0.889
^{1}12f	$D_{\infty h}$	$^1\Sigma_g^+$	m	1.183	1.980				
				1.191		1.963			0.910
^{1}9c	$C_{\infty v}$	$^1\Sigma^+$	TS	1.118	2.470	2.397			0.929
^{3}13a	C_{2v}	$^3A_2$	m	1.141	2.571	2.168	72.7		1.283
^{3}14e	D_{2h}	$^3B_{2g}$	TS	1.315		2.085	36.8		1.321
^{3}19h	D_{2h}	$^3B_{1g}$	TS_2		2.361	1.883	77.6		2.989
^{3}21g	$C_{\infty v}$	$^3\Pi$	m	1.808	1.705	1.812			3.908
^{1}17h	D_{2h}	^1A_g	m		2.228	1.936	70.3		
					2.258	1.931	72.1		3.959
^{1}22g	$C_{\infty v}$	$^1\Sigma^+$	m	1.864	1.691	1.829			3.990
^{3}23h	D_{2h}	$^3B_{1u}$	m		1.926	2.610	85.3		4.545
^{1}28k	$D_{\infty h}$	$^1\Sigma_g^+$	m		2.615	1.678			5.629
^{3}27k	$D_{\infty h}$	$^3\Sigma_g^-$	TS[c]		2.210	1.821			5.861
^{3}25j	C_{2h}	^3B_g	m		2.218	1.833	155.9		
				2.422	1.729	155.9 fixed		5.937	

For some species RCCSD(T) geometries are given as a second row for the pertinent structure. Distances in Ångstrom, angles in degree, T_e's in eV.
[a] m = minimum, TS = transition state, TS_2 = second-order transition state.
[b] Bond length R_3' (Fig. 1).
[c] Two degenerate imaginary linear bends.

Table 9
Bond lengths R_e(Å), dissociation energies D_e (kJ/mol) with respect to the ground state products of Ga_2, N_2 and GaN molecules, harmonic frequencies ω_e (cm^{-1}) and excitation energies T_e (eV) at MP2 and RCCSD(T)/aug-cc-pVTZ levels of theory

Species	MP2				RCCSD(T)			
	R_e	D_e	ω_e	T_e	R_e	D_e	ω_e	T_e
$Ga_2(X^3\Pi)$[a]	2.576	156.4	198	0.0	2.612	150.8	184	0.0
$Ga_2(A^3\Sigma_g^-)$	2.889	284.8	138	4.852	2.902	293.5	133	4.606
$Ga_2(a^1\Sigma_g^+)$	2.869	101.6	145	0.814	2.892	113.3	139	0.389
$GaN(X^3\Sigma^-)$[b]	1.976	248.4	557	0.0	1.990	218.0	539	0.0
$GaN(A^3\Pi)$	1.857	232.0	618	0.170	1.853	211.3	621	0.070
$N_2(X^1\Sigma_g^+)$	1.114	964.9	2187	–	1.104	912.2$_5$	2339	–

[a] R_e = 2.794 Å, DFT data from Refs. [5,6].
[b] R_e = 2.064 Å, D_e = 236.4 kJ/mol, ω_e = 447 cm^{-1}, DFT data from Refs. [5,6].

3.1. In_2N_2

The geometries of the calculated 28 isomers of In_2N_2 dimer are summarized in Table 3. Here the point group symmetry, the irreducible representation, spin multiplicity, and the type of extremum also are given, i.e. whether it is a minimum or a saddle point.

For comparison, calculations have been carried out on the diatomic fragments, In_2, InN and N_2 (Table 4), with the same computational procedure as employed for the dimer. The ground state $X^3\Pi$ of In_2 has a bond length R_e = 3.005 Å and dissociation energy D_e = 199.4 kJ/mol at RCCSD(T)/aug-cc-pVTZ(-PP) level of theory. The first excited state $A^3\Sigma_g^-$ is at 12.1 kJ/mol above the ground state, and it has a shorter bond length by 0.24 Å. The global minimum of the lowest singlet, $a^1\Sigma_g^+$, has an elongated R_e compared to the ground state by 0.29 Å, while there also exists a local minimum (see Table 4) of this state. For the InN molecule the ground state $X^3\Sigma^-$ has R_e = 2.222 Å and D_e = 166.4 kJ/mol. The first excited state, $A^3\Pi$, is at ~20 kJ/mol (0.2 eV) above the ground state and has an R_e value 0.14 Å shorter than the bond distance of $X^3\Sigma^-$. These results may be compared to the best spin–orbit free result of previous RCCSD(T) calculations where $X^3\Sigma^-$ has R_e = 2.206 Å, $A^3\Pi$, is at ~18 kJ/mol above the ground state with R_e of 2.064 Å [38].

Table 10
Ga_2N_2 Dissociation energies D_1 (kJ/mol) with respect to $Ga_2(X^3\Pi) + N_2(X^1\Sigma_g^+)$ for the triplet and $Ga_2(a^1\Sigma_g^+) + N_2(X^1\Sigma_g^+)$ for the singlet structures, D_2 with respect to $2Ga(^2P) + N_2(X^1\Sigma_g^+)$

Species		D_1	D_1 (BSSE)[a]	D_2	D_2 (BSSE)[a]
		$Ga_2 + N_2$		$2Ga + N_2$	
	**^{3}1a**	36.6	5.7	219.9	141.1
		70.7	43.2	175.4	117.7
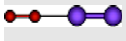	**^{3}3c**	12.8	7.0	196.1	136.4
		53.2	48.0	158.0	118.8
	**^{3}4d**	5.0	1.2	188.3	137.3
		49.3	45.9	154.1	122.6
	**^{1}6a**	69.8	−39.6	174.6	50.8
		114.6	−42.1	140.8	44.4
	**^{1}8d**	0.9	−4.8	105.6	44.2
		80.3	75.2	106.5	65.7
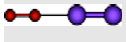	**^{1}9c**	3.9	−28.6	108.7	24.5
		76.4	47.3	102.6	41.5
	**^{3}13a**	[b]	[b]	115.0	−1.4
				68.5	−21.4

For each isomer the first row refers to MP2/aug-cc-pVTZ, the second row refers to RCCSD(T)/aug-cc-pVTZ level of theory.
[a] BSSE-corrected value.
[b] Unbound structure.

3.1.1. $In_2 + N_2$

The **^{3}1a**, **^{3}3c**, **^{3}4d**, **^{3}5d**, **^{1}6a**, **^{1}8d**, **^{1}9c**, and **^{3}13a** structures can be considered as dimers formed by the combination $In_2 + N_2$, i.e. as a result of *intermolecular interaction of two non-polar molecules*. The dissociation energies D_1 with respect to $In_2(X^3\Pi) + N_2(X^1\Sigma_g^+)$ for

Table 11
Ga_2N_2 dissociation energies D_2 (kJ/mol) with respect to $2Ga(^2P) + N_2(X^1\Sigma_g^+)$ fragments

Species		D_2	$D_{2\ (BSSE)}$[a]
		2Ga + N_2	
	^{1}**7e**	212.0	83.6
		192.2	91.8
	^{1}**2b**	204.7	96.6
		171.5	89.2
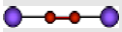	^{3}**10f**	232.3	111.7
		143.8	−18.9
	^{3}**11b**	205.4	88.0
		116.0	25.3
	^{1}**12f**	118.3	0.0
		104.4	59.4
	^{3}**14e**	176.0	48.5
		64.8	−34.8

For each isomer the first row refers to MP2/aug-cc-pVTZ, the second row refers to RCCSD(T)/aug-cc-pVTZ level of theory.
[a] BSSE-corrected value.

Table 12
Ga_2N_2 dissociation energies D_3 (kJ/mol) with respect to 2GaN ($X^3\Sigma^-$) fragments

Species		D_3	$D_{3\ (BSSE)}$[a]
		2GaN	
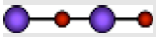	^{3}**21g**	178.5	118.1
		400.3	345.9
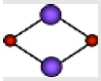	^{1}**17h**	358.7	213.9
		395.4	281.6
	^{3}**27k**	146.9	91.0
		211.8	161.8
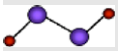	^{3}**25j**	138.4	75.6
		204.5	148.5

For each isomer the first row refers to MP2/aug-cc-pVTZ, the second row refers to RCCSD(T)/aug-cc-pVTZ level of theory.
[a] BSSE-corrected value.

the triplet and $In_2(a^1\Sigma_g^+) + N_2(X^1\Sigma_g^+)$ for the singlet structures of the In_2N_2 molecule and D_2 with respect to $2In(^2P) + N_2(X^1\Sigma_g^+)$ at MP2 and RCCSD(T) level of theory are given in Table 5.

The lowest minimum, ^{3}**1a**, the $^3B_1$ state, is a T-shaped structure of In_2N_2, consisting of a $N_2(X^1\Sigma_g^+)$ molecule which interacts perpendicularly with the In–In bond of the $In_2(X^3\Pi)$ molecule. The BSSE-corrected binding energy of this structure is of 6.3 kJ/mol at the RCCSD(T)/aug-cc-pVTZ(-PP) level. The corresponding binding energy with respect to the $2In(^2P) + N_2(X^1\Sigma_g^+)$ is 115.6 kJ/mol. The In–In bond distance in the ^{3}**1a** dimer is shorter by 0.024 Å than the R_e of the free species, see Tables 3 and 4. The frequency of the In–In and N≡N stretching modes are 127.6 and 2186.2 cm^{-1} in the free $In_2(X^3\Pi)$ and $N_2(X^1\Sigma_g^+)$ molecules respectively, at the MP2/aug-cc-pVTZ(-PP) level of theory. In In_2N_2 both frequencies are blue-shifted: the In–In frequency only slightly (133.5 cm^{-1}) while the N≡N stretching mode (2629.0 cm^{-1}) is blue-shifted by 443 cm^{-1} implying that the N≡N stretching is hindered by the presence of the In_2 molecule, while the stretching of In_2 is practically unaffected.

The ^{3}**3c** isomer is a minimum energy structure consisting of $In_2(A^3\Sigma_g^-) + N_2(X^1\Sigma_g^+)$. The binding energy with respect to these products is 2.7 kJ/mol, while with respect to the diatomic ground states limit it is unbound by 9.4 kJ/mol at the RCCSD(T) level of theory. The stretching mode of $In_2(A^3\Sigma_g^-)$ is calculated at 166.9 cm^{-1} and that of $N_2(X^1\Sigma_g^+)$ at 2186.2 cm^{-1} (see Table 4) and we observe only a slight blue shift in the corresponding frequencies calculated for the dimer (173.7 and 2189.6 cm^{-1}, respectively).

The ^{3}**4d**, ^{3}**5d**, ^{1}**8d**, and ^{1}**9c** species are transition states lying from 11.6 to 58.9 kJ/mol above the global minimum, ^{3}**1a**. The first three are T-shaped structures while the fourth is a linear structure, see Table 3 and Fig. 1. In the first three isomers, their imaginary frequencies correspond to a motion of the N_2 molecule so as to make In_2N_2 linear.

The ^{1}**6a** minimum is a T-shaped structure consisting of $In_2(a^1\Sigma_g^+) + N_2(X^1\Sigma_g^+)$. Structure ^{1}**6a** is unbound with respect to these products, (BE = −18.76 kJ/mol). However, if we take into account the fact that the $a^1\Sigma_g^+$ state of In_2 involved in the dimer is in its local minimum, as shown by the orbitals, population analysis and bond distances, then with respect to the local minimum of $In_2(a^1\Sigma_g^+) + N_2(X^1\Sigma_g^+)$, the binding energy becomes 7.84 kJ/mol. The stretching mode of the $In_2(a^1\Sigma_g^+)$ is 150.1 cm^{-1} in the local minimum and comparing this value and the corresponding value for N_2 stretching with those values of ^{1}**6a** we observe a small blue shift in the mode of In_2 and a red shift in N_2's stretching mode (250.2 and 2021.8 cm^{-1}).

3.1.2. 2In + N_2

The ^{1}**2b**, ^{1}**7e**, ^{3}**10f**, ^{3}**11b**, ^{1}**12f**, and ^{3}**14e** structures can be considered as the result of the interaction of two indium atoms with nitrogen molecule (2In + N_2). Their geometries at MP2 and RCCSD(T) level of theory are given in Table 3. The dissociation energies D_2 with respect to $2In(^2P) + N_2(X^1\Sigma_g^+)$ at MP2 and RCCSD(T) level of theory are given in Table 6. We have not included structure ^{3}**11b** (of Fig. 1) in Table 6 due to unacceptably large t_1 excitation amplitude.

The lowest minimum, ^{1}**2b**, is formed by the N_2 molecule and two In(^{2}P) atoms interacting the first one with the triple bond and the other one with one N atom, see Fig. 1. Moreover, between the two In atoms a bond is formed, resembling the $a^1\Sigma_g^+$ state of In_2, and leading to a cyclic structure for In_2N_2 (see Fig. 1). The In–In distance is ∼3.25 Å at both the MP2 and RCCSD(T) levels of theory. The BSSE-corrected dissociation energy with respect to 2In + N_2 is 85.7 (89.8) kJ/mol and with respect to $In_2(a^1\Sigma_g^+) + N_2$ is 7.3 (0.7) kJ/mol at the MP2 (RCCSD(T)) level of theory.

The ^{1}**7e** minimum is a ^1A_g structure of D_{2h} symmetry and it is the seventh structure lying at 69 kJ/mol above the global minimum at the RCCSD(T) level. It might be noted that the corresponding structure in Ga_2N_2 has been found to be the global minimum (see Section 3.2). In ^{1}**7e**, each In atom interacts with the N_2 molecule and the dissociation energy with respect to the 2In + N_2 products is 28.3 kJ/mol at RCCSD(T) level.

The ^{3}**10f** and ^{1}**12f** minima are lying at about 100 kJ/mol above the ^{3}**1a** global minimum, and their absolute order is reversed in the RCCSD(T) level of theory. They are linear structures; each In atom is connected to an N atom of N_2 molecule. From the population analysis it seems that the N_2 molecule could be excited.

3.1.3. 2InN

The ^{3}**15g**, ^{3}**16h**, ^{1}**17h**, ^{3}**18i**, ^{3}**19h**, ^{3}**20g**, ^{3}**21g**, ^{1}**22g**, ^{3}**23h**, ^{1}**24j**, and ^{1}**26g** species have been formed by combination of two InN molecules. Five of them are linear having an In–N–In–N (**g**) structure, four of them have a rhombic (**h**) structure with a D_{2h} symmetry one is planar (^{3}**18i**) and one has a C_{2h} symmetry (^{1}**24j**), see Table 3 and Fig. 1. All are minima with the exception of the ^{3}**15g**, and ^{3}**19h** species. We have not included structures ^{3}**15g** and ^{1}**26g** in Table 7 due to unacceptably large t_1 excitation amplitudes. It should be noted that in this case, unlike the situation in the **e** species, the rhombic **h** structure does not facilitate any N–N interactions, since the N–N distance is very large (2.7–3.5 Å).

Thus, there are nine species formed by 2InN that are bound with respect to the ground state of two InN with a binding energy ranging from 254 to 119 kJ/mol at the MP2 and from 171 to 71 kJ/mol at the (RCCSD(T)) level of theory (Table 7). For two of them (^{3}**20g**, ^{3}**23h**) we have only RCCSD(T) data since MP2 geometries did not converge. This group exhibits the strongest binding with respect to potential fragments. Concerning the excitation energies, the absolute order is different in MP2 and RCCSD(T) methods for some species of this group, i.e. the ^{1}**17h** (^1A_g, D_{2h} symmetry) in MP2 is low-lying while in RCCSD(T) is lying higher than the ^{3}**19h**, ^{3}**20g**, and ^{3}**21g** structures (Tables 3 and 7).

Summarizing the reliability of the single-reference RCCSD(T) we must quote the largest single (t_1) and double excitation (t_2) amplitudes (Table 2). For the majority of the isomers, the t_1 and t_2 are acceptably small, well below 0.15, with the exception of ^{3}**11b**, ^{3}**15g** and ^{1}**26g** where the t_1 and t_2 are larger than 0.2. The large amplitudes indicate that these isomers possess non-negligible multireference character. Accordingly, we have not included these structures in the analysis of dissociation energies (in Tables 6 and 7).

3.2. Ga_2N_2

The geometries of 22 Ga_2N_2 isomers in various electronic states are listed in Table 8, while the properties of the monomers in various electronic states are given in Table 9. The diatomic fragments Ga_2, GaN and N_2 (Table 9) were calculated at the same computational level as the dimers. There are no spectroscopic experimental data on Ga_2 and GaN molecules, so we can assess the performance of the aug-cc-pvtz basis set only for the ground state of the N_2 molecule. The pertinent experimental data are: R_e = 1.098 Å, ω_e = 2359 cm^{-1}. As expected, MP2 overshoots the experimental R_e and underestimates harmonic frequency. The RCCSD(T) spectroscopic properties of N_2 are in very good agreement with experiment, the differences in R_e and ω_e are below 1%.

The dissociation energies of the structures with respect to three types of products (Eqs. (1)–(3)) are given in Tables 10–12. In contrast to In_2N_2, the lowest energy structure is the rhombic ^{1}**7e**. In Tables 10–12 we have considered also those structures that have very small values of one or two imaginary frequencies. They indicate that the potential energy surface is extremely flat and we can not exclude that they might turn out to be minima with the modifications in the computational method and/or basis set. For instance, optimizing the ^{3}**1a** isomer at the MP2/cc-pvtz and also at the CCSD(T)/cc-pvtz levels lead to the minimum structure, with no imaginary frequencies (see Supplementary material). Optimization of this structure using the counterpoise correction in each optimization step at MP2/aug-cc-pvtz level (see Ref. [39]) also revealed that the resulting stationary point is a minimum. These results clearly show that the vibrational frequencies of a floppy ^{3}**1a** isomer are extremely sensitive to the minute details of the potential energy surface. Based on these results, we treat the ^{3}**1a** isomer as a minimum. Similar arguments can be applied also for the structures ^{3}**3c**, ^{3}**4d**, ^{1}**8d**, ^{1}**9c** and ^{3}**14e**, so we have included all of them in our analysis of dissociation energies.

3.2.1. $Ga_2 + N_2$

In this group we have **a**-, **c**- and **d**-type structures, primarily as a results of the quadrupole–quadrupole interaction of the homonuclear monomers $N_2 + Ga_2$. This interaction modifies the N–N bond only slightly, in contrast to the GaGa bond that varies quite considerably. In this respect, the structures collected in Table 10 can be divided into three groups: triplets (^{3}**4d**, ^{3}**13a**) where there is no change in the GaGa bond, triplets (^{3}**1a**, ^{3}**3c**) where there is an slight contraction of the Ga–Ga bond and singlets (^{1}**6a**, ^{1}**8d** and ^{1}**9c**) with significant contraction of the Ga–Ga bond with respect to the pertinent monomer. Their T_e's are ordered according to this grouping (Table 8), where it might be noted that the highest lying isomer ^{3}**13a** is the first excited state w.r.t. ^{3}**1a** and this excitation actually leads to thermodynamically unstable T-shaped cluster. At the MP2 level the dissociation of the structures ^{3}**1a**, ^{3}**3c** and ^{3}**4d** to homonuclear fragments is endothermic-to-thermoneutral process, while the CCSD(T) data indicate that these structures are thermodynamically stable, though weakly bound van der Waals complexes (Table 10). They possess very weak Ga–N bond(s). In the subset of singlets the MP2 data indicate instability of the complexes w.r.t. homonuclear monomers, while the inclusion of higher excitations in CCSD(T) dissociation energies discriminates between ^{1}**6a** (exothermic w.r.t. $N_2 + Ga_2$) and ^{1}**8d**, ^{1}**9c** – their decomposition is endothermic w.r.t. $N_2 + Ga_2$, similar to triplets.

3.2.2. $2Ga + N_2$

First of all we will discuss the dissociation energies D_2 from Table 10. There is striking distinction between triplets and singlets. For the triplets the dissociation into $2Ga + N_2$ is accompanied with substantially higher energy demand than for the remaining singlets (^{1}**6a**, ^{1}**8d**, ^{1}**9c**). Both the higher order correlation effects and the CP-correction tend to decrease the D_2 values. There are two exceptions for the structures ^{1}**8d** and ^{1}**9c**, the CP-corrected RCCSD(T) values are smaller than MP2 ones. Again, the excited state ^{3}**13a** seems to be unstable also w.r.t. $2Ga + N_2$ fragments. Structures ^{1}**2b**, ^{1}**7e**, ^{3}**10f**, ^{3}**11b** and ^{1}**12f**, collected in Table 11, differ from those in Table 10. In general, one can describe them as species with the nitrogen molecule perturbed by two gallium atoms in various arrangements. They possess no Ga–Ga bond or this bond is substantially elongated compared to the Ga_2 molecule. On the other hand, both gallium atoms can form separate bond with nitrogen atoms. These two factors have opposite effects on D_2 and the resulting dissociation energies do not exhibit sound trends as in Table 10. For instance, except for ^{1}**7e** isomer all CP-corrected CCSD(T) dissociation energies decrease, but in two cases leading even to unbound structures, ^{3}**10f** and ^{3}**14e**. An interesting feature for all structures Table 11 is the relatively large CP-correction indicating substantial geometrical relaxation, compared to the moderate CP-corrections in Table 10.

3.2.3. 2GaN

The thermochemistry of ^{3}**21g**, ^{1}**17h**, ^{3}**27k**, and ^{3}**25j** species, formed from two GaN molecules, is completely different from the previous groups. Structures ^{3}**21g**,^{3}**27k** are linear, ^{1}**17h** is rhombic and ^{3}**25j** is planar. Due to the large t_1 and t_2 amplitudes we have to exclude the structures ^{1}**22g** and ^{3}**23h** from our analysis. All the structures are thermodynamically stable and the first three species in Table 12 possess quite strong Ga–N bonds (central ones for ^{3}**21g** and bifurcated for the rhombic structure). These three isomers are grouped within a relatively small 0.1 eV interval and are by far the most stable species in the Ga_2N_2 family. The remaining two triplets, shifted in T_e higher by ~2 eV are substantially destabilized.

4. Discussion

As mentioned in the Introduction, there are three previous theoretical studies on In_2N_2 with which some of our results can be compared. In the DFT study on In_2N_2 by Cardelino et al. the authors report a series of compounds containing In atoms [7]. Only two of our In_2N_2 isomers, the linear $D_{\infty h}$ ($^3\Sigma_g$) (corresponding to our In–NN–In ^{3}**10f** structure) and the rhombic D_{2h} (^1A_g) (corresponding to our ^{1}**7e**) were examined in [7] using the B3LYP functional and the 3-21G(d,p)$_{In}$ 6-311G(d,p)$_N$ basis augmented with the AKR4 extended basis set. Contrary to our results, they found the linear structure lower than the rhombic. Their geometries are similar to ours. Reversed order of stabilities of analogous linear and rhombic

structures of In_2N_2 was reported in another DFT study, by Kandalam et al. [5]. In fact, when we restrict ourselves to structures investigated in [5] there is some overlap between their DFT and our CCSD(T) results. Nevertheless, their InIn–NN cluster, with the most negative total energy ($C_{\infty v}$, corresponding to our ^{3}**3c** $^3\Sigma^-$ state) has much longer In–N bond than our ^{3}**3c** structure and shows an imaginary frequency, while ours is a minimum. There exist some similarities in the ordering of their five structures with our results. Their rhombic D_{2h} structure, a minimum, has similar geometry as our ^{1}**7e** ^1A_g structure and has energy higher by 0.24 eV than their InIn-NN cluster (our difference, as presented in Table 3, is 0.51 eV). Their linear $D_{\infty h}$ In–NN–In structure (our ^{3}**10f** $^3\Sigma_g^-$ complex) is higher in energy than the rhombic complex by 0.11 eV, while our CCSD(T) results (Table 3) lead to a difference between the two structures of 0.47 eV. However, the similarity ends there as in the present work a different structure has been determined as the absolute minimum, as well as a number of other minima and transition states. Furthermore, the results of some preliminary DFT(B3LYP/LANL2DZ) calculations on In_2N_2, also carried out in the present work were not in agreement with corresponding results of MP2 and RCCSD(T) methods. There are big differences in the absolute stability order of the isomers and in some cases also in geometry. For this reason, such calculations were not employed in the present study.

A detailed study on a number of different geometry structures and different states of In_2N_2 was published very recently [8], when this work was in progress. Six kinds of structures and altogether 20 different symmetry and spin states have been computed. The MRCISD method was combined with a relativistic effective core potential for the core electrons of In and N atoms with the (4s4p1d) basis set for the outer $5s^25p^1$ shells for the In atom and the outer $2s^22p^3$ shell for the N atom. In their work the In 4d electrons are in the core part, whereas in the present work they are included in the valence set (see above). Also, the basis set used in the MRCISD calculations was smaller than ours. It has been shown that the inclusion of the 4d In electrons in the valence set significantly affects the calculated R_e and transition energies of the in InN molecule [38]. Maybe this is the main reason why there are some differences between the results of their study and ours. In some cases their bond distances are more than 0.8 Å larger than ours like in the case of our global minimum, ^{3}**1a**($^3B_1$), where our R_e(In–N) is 3.241 Å at RCCSD(T) level and they found 4.070 Å at the MRCI level. Moreover, there are differences in the absolute ordering of optimized structures and states. Our global minimum ^{3}**1a** is in their study 0.08 eV above a ^{3}**d** ($^3B_1$) structure, their global minimum (T-structure in their notation). However, this ^{3}**d** ($^3B_1$) structure we found at the RCCSD(T) level to be higher in energy. Instead, we found a ^{3}**4d** ($^3B_2$), which has analogous structure but different space symmetry as their ^{3}**d** ($^3B_1$), lying 0.12 eV above our ^{3}**1a** global minimum. Our ^{3}**4d** ($^3B_2$) has, however, one imaginary frequency. Their ^1A_g state (our ^{1}**7e** species) is lying by 0.85 (0.69) eV above the $^3B_1$ (^{3}**1a**) species at the MRCI(MRCI + Q) level while in our case the difference is 0.72 eV. We observe that the Davidson correction improves the MRCI value significantly leading to results closer to our RCCSD(T) values. Finally, in the present work some additional low-lying species like ^{1}**2b** have been calculated, which they did not calculate [8], whereas they report some low-lying isomers which could not be calculated with MP2 for technical reasons. At the RCCSD(T) level these structures were found to be high in energy, for the particular space and spin symmetry reported [8].

There is less data for Ga_2N_2 complexes available in the literature than for In_2N_2 dimers. The only work which allows comparison of relative stabilities and geometries of at least five symmetry and spin states of Ga_2N_2 goes back to Ref. [5]. Our RCCSD(T) global minimum is a rhombic ^{1}**7e** structure (D_{2h}, ^1A_g), as is also reported by Kandalam et al. from their DFT calculations [5]. Geometry parameters are also relatively similar. There is a general agreement that the rhombic structure ^{1}**7e** is a global minimum for Ga_2N_2 [5,9,20]. Restricting the comparison to only five structures optimized by DFT [5], this global minimum is followed by the Ga–NN–Ga $D_{\infty h}$ structure, the GaGa–NN and NGa–NGa $C_{\infty v}$ structures, all three having an imaginary frequency. Only then follows another minimum, N–GaGa–N, $D_{\infty h}$. The order and the character of corresponding four complexes following the global ^{1}**7e** minimum, is different with RCCSD(T): first ranking is the ^{3}**3c** GaGa–NN ($C_{\infty v}$, $^3\Sigma^1$) structure, a transition state, followed by ^{3}**10f** and ^{3}**21g** Ga–NN–Ga ($D_{\infty h}$, $^3\Sigma_g$) and NGa–NGa ($C_{\infty v}$, $^3\Pi$) minima. Finally, there is a high lying ^{3}**27k** N–GaGa–N ($D_{\infty h}$, $^3\Sigma_g$) which has an imaginary frequency but its singlet state counterpart, a ^{1}**28k** complex, is a minimum. Energy separations with respect to the global D_{2h}, ^1A_g minimum of Ga_2N_2 for these five states are 0.35, 0.50, 3.91, and 5.86 eV from RCCSD(T) energies, whereas energy separations for equivalent structures obtained by DFT are 0.17, 0.22, 2.78, and 5.27 eV, respectively. We note, however, that by using both MP2 and CCSD(T) methods we were able to obtain the three minima which are closer to the global minimum than is the ^{3}**3c** GaGa–NN structure. Only 0.17 eV above the global ^{1}**7e** minimum is our T-shaped ^{3}**1a** structure (C_{2v}, $^3B_1$) followed by a ^{1}**2b** (Cs $^1A'$) minimum separated from ^{1}**7e** by 0.21 eV. Many other states, as summarized in Table 8, are energetically in between five structures optimized by DFT.

4.1. Comparison of In_2N_2 and Ga_2N_2

The lowest lying complex of In_2N_2 is the T-type ^{3}**1a** structure (C_{2v}, $^3B_1$) followed by ^{3}**3c** ($C_{\infty v}$, $^3\Sigma^-$), ^{1}**2b** (Cs), ^{1}**6a** (C_{2v}, $^1A_1$) and the ^{1}**7e** (D_{2h}, ^1A_g) complexes, considering minima with no imaginary frequency. This order follows from RCCSD(T) energies. Note that MP2 predicts that the ^{1}**2b** structure is more stable than the ^{3}**3c** structure, see Table 3. A major difference between the stability of Ga_2N_2 and In_2N_2 is that the most stable structure of Ga_2N_2 is the rhombic ^{1}**7e**(D_{2h}, ^1A_g) complex, followed by a T-type structure ^{3}**1a**. Slightly higher are the ^{1}**2b**, ^{3}**10f** ($D_{\infty h}$, $^3\Sigma_g^-$) and ^{1}**6a** minima. However, the T-type structure is only 0.17 eV higher than the global rhombic ^{1}**7e** minimum of Ga_2N_2. Note that the ^{3}**3c** complex, a low-lying minimum in In_2N_2 has an imaginary frequency in Ga_2N_2. The first five minima of the free In_2N_2 molecule are separated from its global ^{3}**1a** minimum by 0.21, 0. 0.29, 0.49, and 0.72 eV, respectively. The first five minima of the free Ga_2N_2 molecule are separated from its global ^{1}**7e** minimum by 0.17, 0.21, 0.50, and 0.53 eV, respectively. The energy separation between lowest minima of Ga_2N_2 is thus slightly smaller than in In_2N_2.

Some analogies between states of In_2N_2 and Ga_2N_2 can be better observed by comparing dissociation energies. The first group of reactions is collected in Tables 5 and 10, respectively, for species which can be considered as complexes between Me_2 and N_2. In D_1 and D_2 energies we consider the dissociation with respect to fragments $Me_2 + N_2$ and with respect to $2Me + N_2$. We see that for both Me_2N_2 species there is a group of Me_2N_2 molecules, ^{3}**1a,** ^{3}**3c**, and ^{3}**4d** which have D_2 dissociation energy about 100 kJ/mol or higher. The dissociation energy of ^{3}**5d** for Ga_2N_2 is omitted since this species has two imaginary frequencies. The picture is less transparent if we consider D_1 dissociation energies. We just note that these energies are generally smaller than are D_2 energies indicating low stability or even instability of Me_2N_2 with respect to the separation to $Me_2 + N_2$ molecules.

Another group of D_2 dissociation energies with respect to $2Me + N_2$ concerns structures represented by N_2 interacting with two Me atoms, see Tables 6 and 11. Aside from the reversed order of stabilities of the ^{1}**7e** and ^{1}**2b** complexes for In_2N_2 and Ga_2N_2, we observe significantly higher D_2 dissociation energies for these two

Table 13
Counterpoise corrected MP2 geometries of the Ga_2N_2 isomers

Species/sym/state/type[a]				R_1	R_2	R_3	ϕ_1	T_e
^{1}**7e**	D_{2h}	^1A_g	m	1.274		2.134	34.7	0.0
^{3}**1a**	C_{2v}	$^3B_1$	m	1.113	2.557	3.115	48.5	0.173
^{3}**3c**	$C_{\infty v}$	$^3\Sigma^-$	TS	1.114	2.438	4.002		0.331
^{3}**4d**	C_{2v}	$^3B_2$	m	1.114	2.579	4.544	14.1	0.372
^{1}**6a**	C_{2v}	$^1A_1$	m	1.120	2.379	2.692	52.4	0.560

RCCSD(T) excitation energies T_e.[b] Distances in Ångstrom, angles in deg, T_e's in eV.
[a] m = minimum, TS = transition state.
[b] Excitation energies calculated at optimized geometries.

structures for both In_2N_2 and Ga_2N_2. Higher D_2 values from both MP2 and RCCSD(T) calculations were found for Ga_2N_2. Besides, the ^{1}**7e** and ^{1}**2b** complexes all other In_2N_2 complexes of this type have negative dissociation D_2 energies. No clear trend could be found for dissociation energies D_3 with respect to MeN ($X^3\Sigma^-$) fragments, see Tables 7 and 12. This is caused partly by difficulties when considering BSSE effects, which are very large particularly for Ga_2N_2.

The BSSE corrections for both In_2N_2 and Ga_2N_2 dimers are relatively large for some dissociation energies presented in Tables 5–7, 10–12. One reason may be a large change of the geometry of the subsystem participating in the particular complex in comparison to the geometry of the isolated species. It should be pointed out that the convergence of the CCSD procedure may be deteriorated when the geometry is far from the equilibrium which may lead to large CC amplitudes. Also, depending on the structure of the complex it happens that due to the presence of the ghost functions the high symmetry of the monomer is lowered. One has to be careful in obtaining the desired spectroscopic state of the monomer calculated in a lower symmetry. Finally, the use of diffuse functions in the augmented basis sets lead typically to the enhancement of BSSE. Augmented basis sets must be used since some of our complexes are Van der Waals species.

To shed more light on the BSSE problem associated with the geometry of Ga_2N_2 isomers we have reoptimized selected low-lying Ga_2N_2 structures with the inclusion of the counterpoise correction in the optimization and frequency calculation (structures ^{3}**1a**, ^{3}**3c**, ^{3}**4d**, ^{3}**5d**, ^{1}**6a**, ^{1}**7e**) [39]. The results are collected in Table 13. Two striking effects of the CP correction were observed: in geometries, it is the elongation of the R_3 coordinate (accompanied by narrowing of the bonding angle ϕ_1) and, for isomers ^{3}**1a** and ^{3}**4d** the change from TS to minimum. The first effect indicates that suppressing the mutual 'borrowing' of the basis functions between the monomers decreases the over binding and, consequently, the inter-monomer distance is larger. The second feature, change in the nature of the stationary point is not surprising since the non-corrected (imaginary) frequencies in ^{3}**1a** and ^{3}**4d** were extremely low (flat potential energy surface), thus the CP-corrected Hessian matrix turned out to positive-definite. The only remaining transition state in this set is ^{3}**3c**, however, the respective imaginary frequencies are extremely low. The excitation energies calculated at these geometries differ only slightly from the corresponding values in Table 8.

5. Conclusions

We have calculated 28 and 22 isomers of the In_2N_2 and Ga_2N_2 molecules, respectively, in various electronic states utilizing the MOLPRO [43] and MOLCAS [44] computer programs. We used the MP2 and RCCSD(T) methods employing the aug-cc-pVTZ and aug-cc-pVTZ-PP basis sets respectively, for the Ga and In atoms and aug-cc-pVTZ for the N atom. Dissociation energies were corrected with respect to the BSSE.

For In_2N_2 our global minimum is a T-shaped C_{2v} $^3B_1$ structure with the N_2 on the C_{2v} axis, which has a dissociation energy of 6.3 kJ/mol with respect to $In_2(X^3\Pi) + N_2(X^1\Sigma_g^+)$ at the RCCSD(T) level of theory. About 0.3 eV above the global minimum four other species are calculated, which are planar, linear NNInIn and T-shaped structures with the In_2 on the C_{2v} axis. The rhombic ^1A_g structure which is the global minimum of the Ga_2N_2 molecule is calculated in the case of In_2N_2 at 0.7 eV above the corresponding global minimum. A T-shaped global minimum of In_2N_2 was also calculated by Cao and Balasubramanian [8], but their main axis is located on the In–In bond.

There is a general agreement [5,20] concerning the global minimum of Ga_2N_2 which is a rhombic D_{2h}, ^1A_g closed-shell complex, in accord with our results. In both cited papers the authors used DFT methods. We were pleased that the dissociation energy, 100 kJ/mol as calculated by Zhou and Andrews [20] – using DFT B3LYP, agrees reasonably well with our RCCSD(T) value, 92 kJ/mol. This agreement does not last, since their DFT calculations predict the $^3\Pi$ as ground state for GaN, which is in disagreement with our result and those of other highly accurate calculations, according to which the ground state of GaN is the $^3\Sigma^-$ state [40]. The global rhombic minimum of Ga_2N_2 is followed by a T-type $^3B_1$ structure separated from the global minimum by only 0.17 eV. The other two minima are 1A', the linear $D_{\infty h}$ $^3\Sigma_g^-$, and the T-shaped C_{2v} $^1A_1$ structures separated from the global minimum by 0.21, 0.50, and 0.53 eV, respectively. While different methods lead to the same global minimum for Ga_2N_2, there is no unambiguous information about the higher lying species.

The dissociation energies calculated in this paper can be assigned to three groups – (a) approximately the smallest were found for $2Me + N_2$ fragments, (b) medium for $Me_2 + N_2$ ones and (c) strongest for MeN fragments. From the point of view of self-assembling monolayers – these clusters may take a part in the initial step of the heterogeneous reaction on suitable surface (e.g. silicon). Then some of the species from the (a) and (b) group may serve as a transfer agents for deposition of the diatomic or triatomic fragments on the surface since it seems easy to release either N_2 or In_2/Ga_2 or In/Ga atom from the cluster. On the other hand – clusters from the (c) group are more firm and may act as stickers for other layers. All these considerations point towards goal-directed adsorption of relevant nitrides with well controlled composition. For the future – it would be interesting to explore also the $Me_2N_2 \rightarrow MeN_2 + Me$ pathways on the Si surface, since they can lead to another class of nitride layers.

Acknowledgements

The support of the Slovak Research and Development Agency (Contract No. APVV-20-018405) and VEGA (Grant No. 1/3560/06) is acknowledged. The authors acknowledge the support from the Greek Secretariat for research and the Slovak Ministry of Education through a Greece–Slovakia bilateral collaboration program.

Appendix A. Supplementary material

Supplementary data associated with this article can be found, in the online version, at doi:10.1016/j.chemphys.2008.02.051.

References

[1] B.F. Levine, Phys. Rev. Lett. 22 (1969) 787.
[2] S. Nakamura, S.F. Chichibu (Eds.), Introduction to Nitride Semiconductor Blue Lasers and Light-Emitting Diodes, Taylor and Francis, London, 2000.
[3] S. Nakamura, S.J. Pearton, G. Fasal, The Blue Laset Diodes, Springer, Berlin, 2000.

[4] H. Morkoc, A. Di Carlo, R. Cingolani, Solid State Electron. 46 (2002) 157.
[5] A.K. Kandalam, R. Pandey, M.A. Blanco, A. Costales, J.M. Recio, J.M. Newsam, J. Phys. Chem. B 104 (2000) 4361.
[6] A. Costales, A.K. Kandalam, A.M. Pendas, M.A. Blanco, J.M. Recio, R. Pandey, J. Phys. Chem. B 104 (2000) 4368.
[7] B.H. Cardelino, C.E. Moore, C.A. Cardelino, D.O. Frazier, K.J. Bachmann, J. Phys. Chem. A 105 (2001) 849.
[8] Z. Cao, K. Balasubramanian, Chem. Phys. Lett. 439 (2007) 288.
[9] A. Costales, R. Pandey, J. Phys. Chem. A 107 (2003) 191.
[10] A.C. Pineda, S.P. Karna, Chem. Phys. Lett. 429 (2006) 169.
[11] L. Andrews, P. Hassanzadech, T.R. Burkoholder, J.M.L. Martin, J. Chem. Phys. 98 (1993) 922.
[12] M. Zhang, Z.M. Su, L.K. Yan, Y.Q. Qiu, G.H. Chen, R.S. Wang, Chem. Phys. Lett. 408 (2005) 145.
[13] S. Nakamura, Science 281 (1998) 956.
[14] P. Waltereit, O. Brandt, A. Trampert, H.T. Grahn, J. Menninger, M. Ramsteiner, M. Reiche, K.H. Ploog, Nature 406 (2000) 865.
[15] S. Vaddiraju, A. Mohite, A. Chin, M. Meyyappan, G. Sumanasekera, B.W. Alphenaar, M.K. Sunkara, Nano Lett. 5 (2005) 1625.
[16] M.C. Johnson, C.J. Lee, E.D. Bourret-Courchesne, S.L. Konsek, S. Aloni, W.Q. Han, A. Zettl, Appl. Phys. Lett. 85 (2004) 5670.
[17] A.F. Belyanin, L.L. Bouilov, V.V. Zhirnov, A.I. Kamenev, K.A. Kovalskij, B.V. Spitsin, Diam. Relat. Mater. 8 (1999) 369.
[18] G. Mattei, Nucl. Instrum. Methods Phys. Rev. B (2002) 191.
[19] B. Song, P.-L. Cao, Phys. Lett. A 382 (2004) 364.
[20] M. Zhou, L. Andrews, J. Phys. Chem. A 104 (2000) 1648.
[21] D. Tzeli, I.D. Petsalakis, G. Theodorakopoulos, Chem. Phys. Lett. 448 (2007) 88.
[22] L.T. Ueno, O. Roberto-Neto, S. Canuto, F.B.C. Machado, Chem. Phys. Lett. 413 (2005) 65.
[23] G. Theodorakopoulos, I.D. Petsalakis, Chem. Phys. Lett. 423 (2006) 445.
[24] M.J. Frisch, G.W. Trucks, H.B. Schlegel, G.E. Scuseria, M.A. Robb, J.R. Cheeseman, J.A. Montgomery Jr., T. Vreven, K.N. Kudin, J.C. Burant, J.M. Millam, S.S. Iyengar, J. Tomasi, V. Barone, B. Mennucci, M. Cossi, G. Scalmani, N. Rega, G.A. Petersson, H. Nakatsuji, M. Hada, M. Ehara, K. Toyota, R. Fukuda, J. Hasegawa, M. Ishida, T. Nakajima, Y. Honda, O. Kitao, H. Nakai, M. Klene, X. Li, J.E. Knox, H.P. Hratchian, J.B. Cross, V. Bakken, C. Adamo, J. Jaramillo, R. Gomperts, R.E. Stratmann, O. Yazyev, A.J. Austin, R. Cammi, C. Pomelli, J.W. Ochterski, P.Y. Ayala, K. Morokuma, G.A. Voth, P. Salvador, J.J. Dannenberg, V.G. Zakrzewski, S. Dapprich, A.D. Daniels, M.C. Strain, O. Farkas, D.K. Malick, A.D. Rabuck, K. Raghavachari, J.B. Foresman, J.V. Ortiz, Q. Cui, A.G. Baboul, S. Clifford, J. Cioslowski, B.B. Stefanov, G. Liu, A. Liashenko, P. Piskorz, I. Komaromi, R.L. Martin, D.J. Fox, T. Keith, M.A. Al-Laham, C.Y. Peng, A. Nanayakkara, M. Challacombe, P.M.W. Gill, B. Johnson, W. Chen, M.W. Wong, C. Gonzalez, J.A. Pople, Gaussian 03 (Revision B.04), Gaussian Inc., Pittsburghs (PA), 2003.
[25] R.J. Bartlett, J.F. Stanton, in: K.B. Lipkowitz, D.B. Boyd (Eds.), Reviews in Computational Chemistry, VCH Publishers, Inc., New York, 1994, p. 65.
[26] D.E. Woon, T.H. Dunning Jr., J. Chem. Phys. 100 (1994) 2975.
[27] Basis Set Exchange, developed by the Collaboratory for Multi-scale Chemical Science (CMCS) in cooperation with EMSL; operated and maintained by EMSL, Pacific Northwest National Laboratory (PNNL), 2006. <http://gnode2.pnl.gov/bse/portal>.
[28] J. Dunning, J. Chem. Soc. 90 (1989) 1007.
[29] K.A. Peterson, J. Chem. Phys. 119 (2003) 11099.
[30] M. Urban, J. Noga, S.J. Cole, R.J. Bartlett, J. Chem. Phys. 83 (1985) 4041.
[31] M. Urban, I. Cernušák, V. Kellö, J. Noga, Methods in Computational Chemistry, Plenum Press, New York, 1987.
[32] R.J. Bartlett, J.D. Watts, S.A. Kucharski, J. Noga, Chem. Phys. Lett. 165 (1990) 513.
[33] J. Paldus, X. Li, Adv. Chem. Phys. 14 (1999) 35.
[34] G. Karlström, R. Lindh, P.-A. Malmqvist, B.O. Roos, U. Ryde, V. Veryazov, P.-O. Widmark, M. Cossi, B. Schimmelpfennig, P. Neogrady, L. Seijo, Comput. Mater. Sci. 28 (2003) 222.
[35] S.F. Boys, F. Bernardi, Mol. Phys. 19 (1970) 553.
[36] D. Tzeli, A. Mavridis, S.S. Xantheas, J. Phys. Chem. A 106 (2002) 11327.
[37] P. Neogrády, M. Medved, I. Cernušák, M. Urban, Mol. Phys. 100 (2002) 541.
[38] L. Demovic, I. Cernusak, G. Theodorakopoulos, I.D. Petsalakis, M. Urban, Chem. Phys. Lett. 447 (2007) 215.
[39] S. Simon, M. Duran, J.J. Dannenberg, J. Chem. Phys. 105 (1996) 11024.
[40] P.A. Denis, K. Balasubramanian, Chem. Phys. Lett. 423 (2006) 247.
[41] I. Johansson, U. Litzén, Ark. Fys. 34 (1967) 573.
[42] B. Roos, P.-A. Malmqvist, Phys. Chem. Chem. Phys. 6 (2004) 2919.
[43] H.-J. Werner, P.J. Knowles, R. Lindh, F.R. Manby, M. Schütz, P. Celani, T. Korona, G. Rauhut, R.D. Amos, A. Bernhardsson, A. Berning, D.L. Cooper, M.J.O. Deegan, A.J. Dobbyn, F. Eckert, C. Hampel, G. Hetzer, A.W. Lloyd, S.J. McNicholas, W. Meyer, M.E. Mura, A. Nicklass, P. Palmieri, R. Pitzer, U. Schumann, H. Stoll, A.J. Stone, R. Tarroni, T. Thorsteinsson, MOLPRO, version 2006.1, a package of ab initio programs.
[44] K. Anderson, M. Barysz, A. Bernhardsson, M.R.A. Blomberg, D.L. Cooper, M.P. Fülscher, C. de Graaf, B.A. Hess, G. Karlström, R. Lindh, P.A. Malmqvist, T. Nakajima, P. Neogrády, J. Olsen, B.O. Roos, B. Schimmelpfennig, M. Schütz, L. Seijo, L. Serrano-Andrés, P.E.M. Siegbahn, J. Stålring, T. Thorsteinsson, V. Veryazov, P.O. Widmark, MOLCAS Version 6.5, Lund University, Sweden, 2002.